JOURNAL OF CHEMICAL & ENGINEERING DATA

ARTICLE

pubs.acs.org/jced

Equilibrium Phase Densities, Vapor Phase Compositions, and Interfacial Tensions for the Methane + Ethane + *n*-Pentane System at 294.15 K

Hui N. Nilssen,[*,†] Arne O. Fredheim,[‡] Ole J. Berg,[‡] Even Solbraa,[‡] and Bjørn Kvamme[§]

[†]Norwegian University of Science and Technology, Kolbjørn Hejes v 1B, 7491 Trondheim, Norway
[‡]Statoil Research Center, Arkitekt Ebbellsvei 10, N-7053 Ranheim, Norway
[§]University of Bergen, Allegaten 55, N-5007 Bergen, Norway

ABSTRACT: The equilibrium phase densities, vapor phase compositions, and interfacial tensions of the ternary mixture (methane + ethane + *n*-pentane) have been measured simultaneously using the pendant drop technique at 294.15 K. The total mole compositions of the measured ternary mixtures are 50.61 % methane + 8.93 % ethane + 40.46 % *n*-pentane; 34.20 % methane + 6.04 % ethane + 59.76 % *n*-pentane; and 17.46 % methane + 3.08 % ethane + 79.40 % *n*-pentane, respectively. The measured phase densities and vapor phase compositions are compared with calculated equilibrium properties from the GERG2004 equation. No open interfacial tension data for these ternary systems have been reported at any isothermal conditions. The average experimental interfacial tension data can be described with the total deviations of about 3.2 %. The combined standard uncertainty at each experimental condition is calculated on the basis of ISO recommendations.

1. INTRODUCTION

The definition of surface tension can manifest itself in forms of both surface energy as well as surface force. In the high-pressure gas−liquid separation systems, the magnitude of interfacial forces in comparison with the gravity could have a direct impact on whether the liquid droplet will be separated from gas flows. Furthermore, the reliable surface tension data are also a key parameter for the accurate simulation of droplet−droplet interactions and droplet−liquid film interactions which can give detailed pictures of the coalescence, deposition, and entrainment phenomena in the separation conditions.

Without any doubt, there is still a paucity of available interfacial tension data for the hydrocarbon systems in the open literature. In this study, the interfacial properties of the methane + ethane + *n*-pentane system are investigated and utilized to mimic the thermodynamic behaviors of a real gas condensate in the high-pressure gas−liquid scrubber. In the earlier study, the interfacial tensions and equilibrium phase densities of the binary mixture (ethane + *n*-pentane) were investigated.[10] In this work, bulk phase densities, vapor phase compositions, and interfacial tensions of the methane + ethane + *n*-pentane system will be measured at 294.15 K. The online Gas Chromatography cell is applied to measure the vapor phase compositions at high-pressure conditions, and about ten samplings will be taken at each experimental condition. The interfacial tension data will be used to form the basis of one future publication about correlation of the numerical model for accurate computation and characterization of the interfacial properties.

2. EXPERIMENTAL APPARATUS AND PROCEDURES

2.1. Experimental Apparatus. In this study, the interfacial tension of a vapor−liquid interface is determined by using a video-enhanced pendant drop tensiometer and axisymmetric drop shape analysis.[1−9] The main components of the experimental system are illustrated in Figure 1. The technical information of the apparatus used in the present measurements has been described in detail previously.[10] The improvement of the experimental rig is the installation of the gas chromatographic (GC) cell. The temperatures of the sampling valves and heating transfer line are set to 160 °C, and it aims that all the sampling is totally vaporized when it reaches the column. The liquid phase sampling is not stable due to the local pressure temperature (PT) flash that is happening at the end of the sampling capillary; it causes the liquid phase composition fluctuations, but the analysis of the vapor phase compositions is very stable and representative. The ten samplings were taken at each experimental condition. The configuration and operating conditions of the online GC cell can be found in Table 1. The response factor formula of methane, ethane, and *n*-pentane components can be found in Table 2.

2.2. Experimental Procedure. *2.2.1. Experimental Uncertainty: Temperature, Pressure, Density, and Composition.* The gas pressure gauge and temperature sensors are already calibrated beforehand by the manufacturer. The temperature sensors are integrated in the high-pressure densitometers. Liquid and vapor densities are determined in an Anton Paar DMA HPM unit based on the vibrating U-tube method. The apparatus measures the oscillating period of the U-tube filled with sample that is automatically converted to phase density after proper calibration. Two calibration fluids, methane and *n*-pentane, have to be selected for calibrations at pressures ranging from (1 to 115) bars and the temperature interval (20.5 to 21.5) °C. The position of the gas densitometer is standing, and the liquid densitometer is lying on the platform. The estimated accuracies are recorded in Table 3.

Received: March 31, 2011
Accepted: September 9, 2011
Published: October 13, 2011

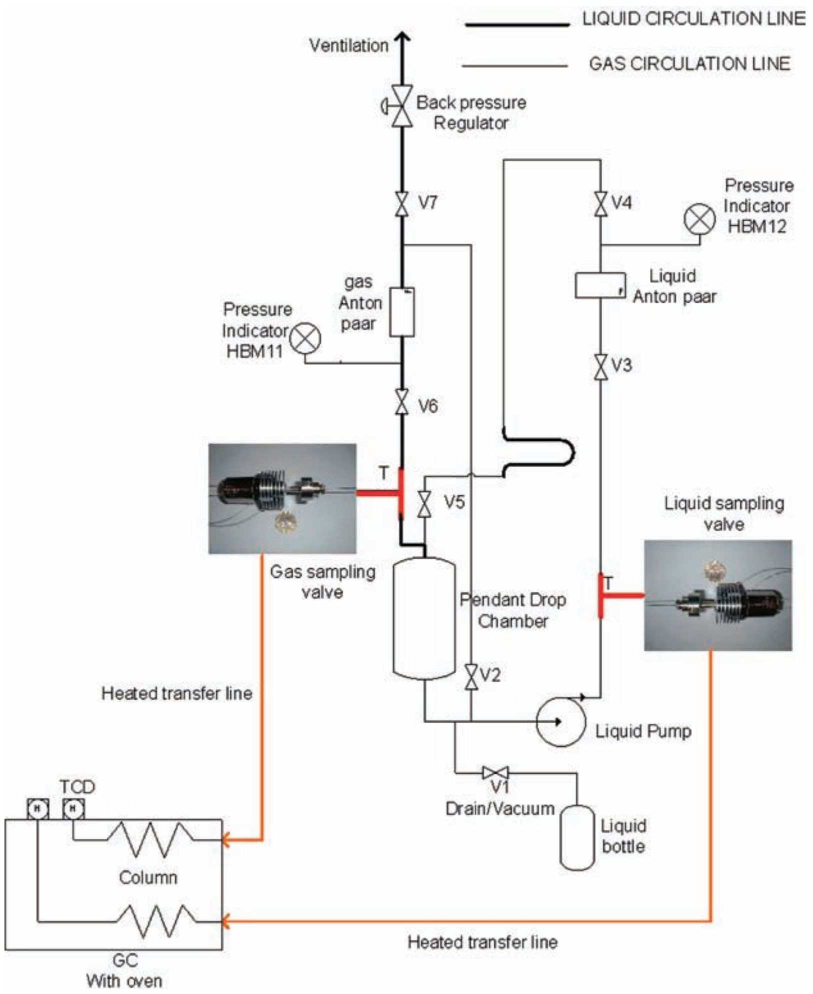

Figure 1. Experimental apparatus (showing the vapor and liquid circulation path).

Table 1. Online Gas Chromatograph Configuration and Operating Conditions

configurations	
injector	ROLSI (Rapid Online Sampler-Injector); electromagnetic
column	length: 120 cm
diameter: 1/8"	
type: Haysep D	
carrier gas	helium
operating conditions	
carrier gas inlet pre. [MPa]	0.083
injector temp. [°C]	160
injection time [s]	0.3
column temp. [°C]	160
thermal detector temp. [°C]	160

Table 2. Response Factor of the Methane, Ethane, and *n*-Pentane

component	response factor
Methane	
$P \leq 2.2$ [MPa]	$0.01367 \cdot P + 0.065006$
$2.2 < P \leq 5.2$ [MPa]	$0.00456 \cdot P + 0.085241$
$5.2 < P \leq 9.2$ [MPa]	$0.00122 \cdot P + 0.102518$
Ethane	
$P \leq 5.2$ [MPa]	$0.01926 \cdot P + 0.093983$
$2.2 < P \leq 5.2$ [MPa]	$0.00693 \cdot P + 0.121345$
$5.2 < P \leq 9.2$ [MPa]	$0.00162 \cdot P + 0.148846$
n-Pentane	
whole pressure range	0.29

2.2.2. Materials. The gas mixture with 85.2 mol % methane + 14.8 mol % ethane was supplied by YARA Industrial AS with a certificate no.: 83399005-01-K-40-5427. The *n*-pentane was supplied by LAB SCAN Limited with a reported purity of 99 mol % (Code No.: A40A11X, Batch No.: 4336/8). No further purification of the chemicals was attempted. The ternary mixture was weighted and stored into a cylinder bottle with pressure up to 170 bar. The total mole compositions of the ternary mixture are listed in Table 4.

2.2.3. Measurement Process. The predetermined amount of ternary liquid mixture from the liquid sample cylinder is filled into the pendant drop cell via valve 1 (see Figure 1), and the valves 2, 5, 6, and 7 were closed before filling. After filling is

Table 3. Estimated Experimental Accuracy

temperature	± 0.1 °C
pressure	0.1 % of reading pressure [MPa]
liquid density	$\pm 4.3 \cdot 10^{-3}$ g·cm^{-3}
vapor density	$\pm 4.4 \cdot 10^{-3}$ g·cm^{-3}
composition	relative 3 % of measuring composition [mol %]

Table 4. Total Mole Compositions of the Ternary System [%]

component	mixture 01	mixture 02	mixture 03
methane	50.61	34.20	17.46
ethane	8.93	6.04	3.08
n-pentane	40.46	59.76	79.46

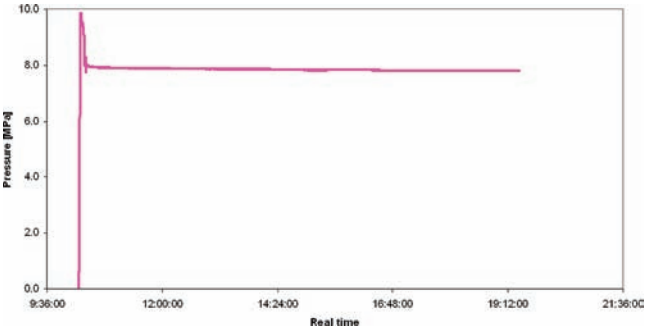

Figure 2. Pressure log data of the ternary mixture: 50. 61 % methane + 8.93 % ethane + 40.46 % *n*-pentane. Pink line, liquid phase pressure.

finished, first valve 5 will be opened cautiously, and the pressure will fall down several bars depending on the ternary mixture compositions and total cell volume. In addition, the gas will flash out from the liquid phase causing small a pressure drop too. The fluid will be circulated from the bottom to the top of the pendant drop cell with the help of the high-pressure liquid pump through the whole liquid circulation path. At last, valves 6 and 7 will be opened to release the flashed gas mixture flow to the gas circulation line, and valve 2 before the liquid pump will be open. The gas mixture will be mixed due to the overpressure of the liquid circulation pump, which can drag the *n*-pentane component in the gas mixture from the bottom of the interfacial tension cell to the whole gas circulation line. It makes fluids more homogeneous and measurement conditions more close to the ideal gas—liquid equilibrium state. Figure 2 shows the example pressure data of the experimental rig. The mixture was filled into the cell at about 10 a.m. up to 100 bar, and the pressure was stabilized at 79 bar at 4 p.m. When both phase pressures and temperatures become stable, the gas samplings will be injected into the GC column ten times. Afterward, the drop will be made and hanged inside in the pendant drop cell; interfacial tensions are calculated from the droplet initial shape analysis.

3. EXPERIMENTAL RESULTS AND DISCUSSION

The measured data for the methane + ethane + *n*-pentane system are listed in Tables 5, 6, and 7 which include the measured phase densities, vapor phase compositions, and interfacial tensions.

Table 5. Comparison of Experimental and Calculated Phase Densities for Methane + Ethane + *n*-Pentane at 294.15 K

pressure	phase density/[g·cm^{-3}]		deviation
[MPa]	experimental	calculated (GERG2004)	(%)
50.61 % methane + 8.93 % ethane + 40.46 % *n*-pentane			
Liquid Phase			
6.395	0.5440	0.5419	−0.4
7.021	0.5440	0.5321	−2.2
7.762	0.5255	0.5200	−1.0
	Average		−1.2
Vapor Phase			
6.395	0.0587	0.0578	−1.5
7.021	0.0650	0.0645	−0.8
7.762	0.0738	0.0729	−1.2
	Average		−1.2
34.20 % methane + 6.04 % ethane + 59.76 % *n*-pentane			
Liquid Phase			
3.596	0.5826	0.5848	0.4
3.681	0.5811	0.5837	0.5
4.066	0.5773	0.5791	0.3
4.093	0.5767	0.5787	0.4
4.354	0.5744	0.5755	0.2
4.597	0.5711	0.5724	0.2
	Average		0.3
Vapor Phase			
3.596	0.0300	0.0300	0.0
3.681	0.0307	0.0308	0.4
4.066	0.0341	0.0341	0.1
4.093	0.0347	0.0343	−1.1
4.354	0.0369	0.0366	−0.7
4.597	0.0394	0.0388	−1.6
	Average		−0.6
17.46 % methane + 3.08 % ethane + 79.46 % *n*-pentane			
Liquid Phase			
1.502	0.6063	0.6099	0.6
1.611	0.6061	0.6089	0.5
1.701	0.6045	0.6079	0.6
1.869	0.6033	0.6063	0.5
1.953	0.6019	0.6054	0.6
2.025	0.6018	0.6047	0.5
	Average		0.5
Vapor Phase			
1.502	0.0123	0.0126	2.7
1.611	0.0136	0.0134	−1.1
1.701	0.0136	0.0141	3.6
1.869	0.0155	0.0154	−0.5
1.953	0.0158	0.0160	1.5
2.025	0.0169	0.0166	−1.8
	Average		1.2

According to Table 5, the calculated average liquid density deviation is −1.2 %, 0.3 %, and 0.5 % for each methane + ethane +

Table 6. Comparison of Experimental and Calculated Vapor Phase Composition for Methane + Ethane + *n*-Pentane at 294.15 K

pressure	vapor phase composition [mol %]						deviation		
	experimental			calculated (GERG 2004)			(%)		
[MPa]	methane	ethane	n-C$_5$	methane	ethane	n-C$_5$	methane	ethane	n-C$_5$
50.61 % methane + 8.93 % ethane + 40.46 % *n*-pentane									
6.395	89.37	8.02	2.61	89.78	7.60	2.62	0.5	−5.2	0.4
7.021	89.43	7.89	2.67	90.00	7.31	2.68	0.6	−7.4	0.4
7.762	89.76	7.43	2.80	90.18	7.02	2.80	0.5	−5.5	0.0
			Average				0.5	−6.0	0.3
34.20 % methane + 6.04 % ethane + 59.76 % *n*-pentane									
3.596	90.24	6.92	2.84	90.57	6.56	2.87	0.4	−5.2	1.1
4.066	90.60	6.67	2.72	91.10	6.16	2.75	0.6	−7.6	1.1
4.354	90.98	6.35	2.66	91.37	5.94	2.69	0.4	−6.5	1.1
			Average				0.4	−6.4	1.1
17.46 % methane + 3.08 % ethane + 79.46 % *n*-pentane									
1.611	89.46	5.80	4.74	89.59	5.75	4.66	0.1	−0.9	−1.7
1.869	90.02	5.65	4.32	90.55	5.27	4.19	0.6	−6.7	−3.0
2.025	90.65	5.32	4.03	91.02	5.01	3.96	0.4	−5.8	−1.7
			Average				0.4	−4.5	−2.1

Table 7. Experimental Interfacial Tensions for the Methane + Ethane + *n*-Pentane System at 294.15 K

pressure	experimental interfacial tension	deviation		
[MPa]	[mN·m^{-1}]	e_1/[mN·m^{-1}]	e_2/[mN·m^{-1}]	$(e_1 + e_2)$/Exp./(%)
50.61 % methane + 8.93 % ethane + 40.46 % *n*-pentane				
6.395	5.9	0.10	0.11	3.5
7.021	5.1	0.04	0.07	2.2
7.762	4.3	0.05	0.07	2.9
34.20 % methane + 6.04 % ethane + 59.76 % *n*-pentane				
3.596	9.9	0.15	0.36	5.1
4.066	9.3	0.10	0.15	2.7
4.354	8.8	0.08	0.14	2.5
17.46 % methane + 3.08 % ethane + 79.46 % *n*-pentane				
1.611	12.8	0.11	0.24	2.7
1.869	12.6	0.16	0.20	2.9
2.025	12.4	0.11	0.18	2.4
	Average			3.2

n-pentane mixture which are listed in Table 4, and the average vapor phase is −1.2 %, −0.6 %, and 1.2 % in comparison with computed results from the GERG2004 equation.[11] The accuracy of the vapor phase density measurement is significantly improved because of the realization of gas mixing in the rig. In the Figure 3 are plotted the experimental phase densities and calculated densities by the GERG2004 equation. In addition, the measured and calculated vapor compositions of methane and *n*-pentane components are plotted separately in Figures 4 and 5. The measured vapor phase compositions are found in Table 6. It can be seen that the average experimental deviations of *n*-pentane in the vapor phase are lower than 2.1 % compared with the GERG2004 equation. The average ethane composition deviation is below 6.4 %. Due to the fact that the concentration of *n*-pentane in the gas phase is relatively very low, a large amount of gas needs to be injected into the column to obtain a stable *n*-pentane peak, and it could cause the methane to be oversaturated in the column and the methane peak to overlap the ethane peak in GC analysis. Because the ethane has a much lower mole percent than methane, the not "ideal" separation has a bigger impact on the ethane composition analysis than methane and causes the high deviation of ethane composition in the GC analysis. However, the dew point temperature is mainly determined by the *n*-pentane composition in the vapor phase, and by verifying the dew point temperature with the vapor phase compositions, it is proved that the dew point temperature is very close to the experimental temperature 21 °C. The experimental condition is very close to the gas−liquid equilibrium state.

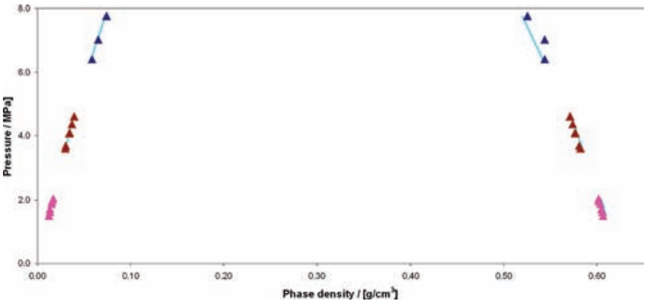

Figure 3. Phase densities for the methane + ethane + *n*-pentane system at 294.15 K. Blue triangle, ternary mixture 01; red triangle, ternary mixture 02; pink triangle, ternary mixture 03; blue line, calculated density by GERG2004.

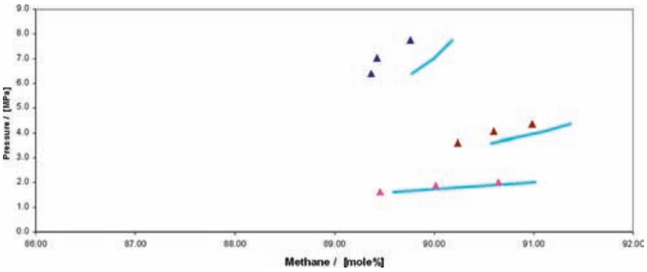

Figure 4. Methane in the vapor phase for the methane + ethane + *n*-pentane system at 294.15 K. Blue triangle, ternary mixture 01; red triangle, ternary mixture 02; pink triangle, ternary mixture 03; blue line, calculated density by GERG2004.

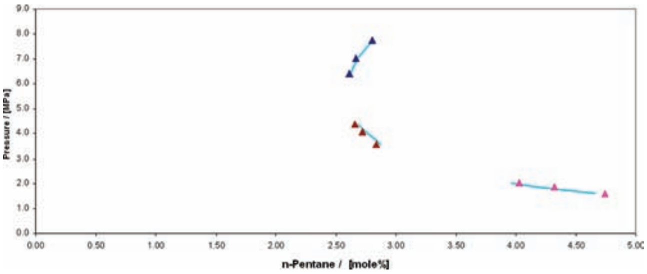

Figure 5. *n*-Pentane in the vapor phase for the methane + ethane + *n*-pentane system at 294.15 K. Blue triangle, ternary mixture 01; red triangle, ternary mixture 02; pink triangle, ternary mixture 03; blue line, calculated density by GERG2004.

In Table 7 are data pertaining to interfacial tension measurements. The total deviation of measurement is made up of two parts. One is uncertainty based on drop shape analysis at each taken picture which can be calculated based on eq 1: N is the total number of pictures which are taken at every experimental condition, and the symbol $\bar{\sigma}$ is the average interfacial tension at each measuring condition.

$$e_1(\sigma) = \sqrt{\frac{1}{N}\sum_{i=1}^{N}(\sigma_i - \bar{\sigma})^2} \qquad (1)$$

The other deviation is the combined standard uncertainty related to the measured phase densities, shape factor, and apex radius. According to ISO recommendations of the combined standard uncertainty calculation,[12] the combined standard uncertainty of the measured interfacial tensions can be computed

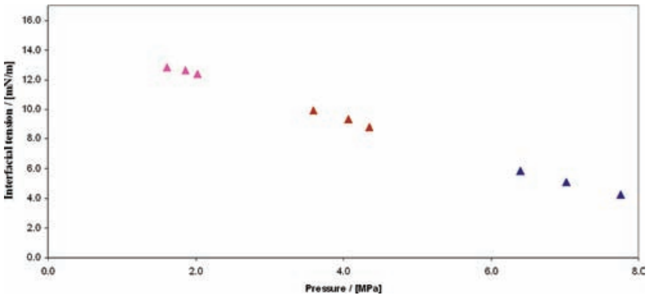

Figure 6. Interfacial tensions for the methane + ethane + *n*-pentane system at 294.15 K. Blue triangle, ternary mixture 01; red triangle, ternary mixture 02; pink triangle, ternary mixture 03.

based on the following equation

$$e_2(\sigma) = \sqrt{\left(\frac{\partial\sigma}{\partial\rho_{\mathrm{liq}}}e(\rho_{\mathrm{liq}})\right)^2 + \left(\frac{\partial\sigma}{\partial\rho_{\mathrm{vap}}}e(\rho_{\mathrm{vap}})\right)^2 + \left(\frac{\partial\sigma}{\partial\beta}e(\beta)\right)^2 + \left(\frac{\partial\sigma}{\partial R_0}e(R_0)\right)^2} \qquad (2)$$

It is shown in Table 7 that the average deviation is 3.2 % for all methane + ethane + *n*-pentane mixtures. For the methane + ethane + *n*-pentane system, no open interfacial tension data have been reported. The experimental interfacial tension versus the pressure is plotted in Figure 6. The measured interfacial tensions decrease with the increasing pressure. The trend is slightly different for all three ternary mixtures due to composition difference. The lowest measured interfacial tension value is about 5.9 mN/m. Because of the limitation of the total cell volume, only three pressure conditions are measured for each ternary mixture. The extension of the cell volume is the next work of focus which makes it possible to measure the interfacial tension at the whole two-phase region.

4. CONCLUSIONS

New data of experimental phase densities and interfacial tensions have been collected for methane + ethane + *n*-pentane at 294.15 K. The accuracy of the liquid and vapor phase density data is in good agreement with PT flash simulation results from the GERG2004 equation. Even though there are high deviations of measured vapor compositions of ethane, the gas—liquid equilibrium is proved to be good by using the vapor phase compositions to verify the dew point temperature which is very close to the experimental temperature. It can be noticed that the deviations of the experimental interfacial tensions are well distributed, and no systematic error exists in our experimental process. In this work, the newly acquired experimental data for methane + ethane + *n*-pentane extend the thermodynamic property database and are useful for the development and verification of the interfacial tension simulation for real gas condensate for high-pressure gas—liquid separation systems.

■ AUTHOR INFORMATION

Corresponding Author

*Tel.: +47 47331575. E-mail: hui.nie.nilssen@ntnu.no.

Funding Sources

The Norwegian Reach Council is gratefully acknowledged for the financial support of H. N. Nilssen's PhD fellowship through the project HiPGLS (169477).

REFERENCES

(1) Hansen, F. K.; Rodsrun, G. Surface tension by pendant drop 1. A fast standard instrument using computer image analysis. *Colloid Interface Sci.* **1991**, *141* (No. 1), 1–9.

(2) Hansen, F. K. Surface Tension by Image Analysis: Fast and Automatic Measurements of Pendant and Sessile Drops and Bubbles. *J. Colloid Interface Sci.* **1993**, *160*, 209–217.

(3) Shi-Yow, L.; Li-Jen, C.; Jia-Wen, X.; Wei-Jiunn, W. An Examination on the Accuracy of Interfacial Tension Measurement from Pendant Drop Profiles. *Langmuir* **1995**, *11*, 4159–4166.

(4) Song, B. H.; Springer, J. Determination of Interfacial-Tension from the Profile of a Pendant Drop Using Computer-Aided Image Processing 1. Theoretical. *J. Colloid Interface Sci.* **1996**, *184* (1), 64–76.

(5) Song, B. H.; Springer, J. Determination of Interfacial-Tension from the Profile of a Pendant Drop Using Computer-Aided Image Processing 2. Experimental. *J. Colloid Interface Sci.* **1996**, *184*, 77–91.

(6) Lahooti, S.; del Río, O. I.; Cheng, P.; Neumann, A. W. In *Applied Surface Thermodynamics*; Neumann, A. W., Spelt, J. K., Eds.; Marcel Dekker Inc.: New York, 1996; Chapter 10.

(7) Hoorfar, M.; Neumann, A. W. Axisymmetric Drop Shape Analysis (ADSA) for measuring surface tension and contact angle. *J. Adhes.* **2004**, *80* (No. 8), 727–743.

(8) Hoorfar, M.; Kurz, M. A.; Neumann, A. W. Evaluation of the surface tension measurement of Axisymmetric Drop Shape Analysis (ADSA) using a shape parameter. *Colloids Surf. A: Physicochem. Eng. Aspects* **2005**, *260*, 277–285.

(9) Hoorfar, M.; Neumann, A. W. Recent progress in Axisymmetric Drop Shape Analysis (ADSA). *Adv. Colloid Interface Sci.* **2006**, *121*, 25–49.

(10) Nilssen, H. N.; Fredheim, A. O.; Berg, O. J.; Solbraa, E.; Kvamme, B. Equilibrium Phase Densities, Interfacial Tensions for the Ethane + n-Pentane System at 294.15 K. *J. Chem. Eng. Data* **2011**, *56*, 2128–2132.

(11) Kunz, O.; Klimeck, R.; Wagner, W.; Jaeschke, M. Technical Monograph: The GERG-2004 Wide-Range Equation of State for Nature Gases and Other Mixtures, GERG TM15 2007.

(12) Uncertainty of measurement-part 3: Guide to the expression of uncertainty in measurement (GUM: 1995), ISO/IEC GUIDE98-3:2008(E).